Acoustics'08 Paris
June 29-July 4, 2008
www.acoustics08-paris.org

Numerical modeling of Panphonics's G1 flat loudspeaker

Krisztián Gulyás and Fülöp Augusztinovicz

Budapest University of Technology and Economics, BME Dept. of Telecommunications,
Magyar tudósok körútja 2, H-1117 Budapest, Hungary
gulyas@hit.bme.hu

The basic idea behind AABC (Active Acoustic Barrier Control) is to reduce the sound radiation of a structure acoustically without influencing the vibration behaviour of the structure. The large surface acoustic polymer material actuator/sensor systems are primarily meant to form the actuator/sensor system for the AABC concept. The main component of this package is a special active device: the rEMA – revised Elastic Mass Actuator based on the Panphonics' G1 panel loudspeaker element. This paper deals with the modelling and the low-frequency performance issues of the G1 flat loudspeaker. The aim was to create an accurate mathematical model to understand the operational principles of the loudspeaker, and then this model was used to optimize its low-frequency performance. Due to the special structure and the optimization tasks, a new numerical method was developed to model special multi-layer coupled vibroacoustics systems based on the Finite Difference and Boundary Element Method. The investigation focuses on the mechanical behaviour of the panel and describes the sound radiation properties also. The performed work was a part of the research of the project InMAR (Intelligent Materials for Active Noise Reduction) which was funded by the European Union.

1 Introduction

Active acoustic applications are still very seldom in commercial and civil life due to the technological problems of audio elements, such as size and weight. In the recent years many new promising materials have been developed and used in various applications. One of these devices is the Panphonics' G1 flat and light-weight loudspeaker/sensor.

The aim of the research was to develop an active sound insulation package that is able to increase sound transmission loss of the car steel structure and thus attenuate the interior noise field by active means. The concept is called "Active Acoustic Barrier Control (AABC)". The main component of this package is a special active device: the EMA – Elastic Mass Actuator based on the Panphonics' G1 flat loudspeaker element. The EMA sound package (at this stage) consists of two G1 flat panel: one is the actuator and another one is the sensor.

In order to optimize the EMA sound package behaviour, further investigation of G1's operation phenomena was needed. In this paper a special modelling method will be described which is capable to model the vibration and the radiation behaviour of complex vibroacoustic structures such as the G1 loudspeaker/sensor.

2 Modelling basics

The behaviour of the complex vibroacoustic structures can be described and determined by their differential equations and the corresponding boundary conditions. However, these equations can be solved in many (simple) case, generally it is difficult (nearly impossible) to determine the unknown functions in explicit form. Thus, many numerical methods have been developed to solve differential equations approximately. Here two numerical methods will be used: the finite difference and the boundary element method. The described methods assume a set of discrete function space as the arguments of the unknown spatial functions e.g. the unknown functions will be determined only at the given points.

Finite difference method calculates the values of the given derivative function at the given points using the difference of the adjacent points. Thus the original differential equations can be transformed into difference equations, which can be reordered and formulated as a matrix equation. Solving of matrix equation is a quite straightforward procedure, limited only by the computation capacity of the selected numerical software/hardware.

2.1 Vibroacoustic Structure

The described numerical concept assumes different layers (structural and acoustical ones), connections between and boundary conditions for each of them. The following layer types are considered: plate, acoustic enclosure and air in porous layers. The thickness of the layers can be different, but their x and the y dimensions are equal, and all of them have squared shape. Between the layers, various boundary conditions can be defined.

The vibroacoustic behaviour of each layer can be described by the partial differential equation (PDE) of the corresponding layer. Since only time-harmonic solution is considered, the governing equations are transformed into frequency domain. The following layers/equations can be defined:

Plate The PDE of a square shaped plate with pretension T can be formulated as [1]

$$\left(D\nabla^4 - T\nabla^2 - \omega^2\rho h\right) u_z(\boldsymbol{r}) = f(\boldsymbol{r}) \;, \qquad (1)$$

where $u_z(\boldsymbol{r})$ is the z directional displacement of the plate and $f(\boldsymbol{r})$ is the acting force at the given $\boldsymbol{r}$ spatial point; D defined as $D = \frac{Eh^3}{12(1-\nu^2)}$, where E is the Young's modulus, ν is the Poisson's ratio, and ρ is the density of plate's material; h stands for the thickness of the plate.

Air gap The spatial pressure function of the air in an acoustic enclosure is described by the well-known Helmholtz equation

$$\left(\nabla^2 - \omega^2\left(-\frac{\rho}{\kappa p_0}\right)\right) p(\boldsymbol{r}) = 0 \;, \qquad (2)$$

where $p(\boldsymbol{r})$ is the pressure at the spatial point $\boldsymbol{r}$, ρ is the density, κ is the specific heat capacity and p_0 is the static pressure of air.

Porous layer The pressure distribution in the homogeneous porous material at low frequencies can be described by the following equation [2]

$$\left(\nabla^2 - j\omega\sigma\phi\frac{1}{\kappa p_0}\right)p(\boldsymbol{r}) = 0\ , \tag{3}$$

where, σ is the specific flow resistivity, ϕ is the porosity of the porous material and the others as above.

2.2 Finite Estimation

As mentioned, the theory is based on the assumption that the argument of the (unknown) functions are discretized, e.g. all of the corresponding functions are represented with their sampled values. Let us consider $f(x)$ as a scalar-valued function over the $[0\ L]$ interval. Divide this interval into N points ($N-1$ segments) and define the vector of the function arguments over the selected interval as

$$\begin{aligned}\mathbf{x} &= \begin{bmatrix}x_0 & x_1 & \dots & x_{N-1}\end{bmatrix}^{\mathsf{T}} \\ &= \Delta x \underbrace{\begin{bmatrix}0 & 1 & \dots & N-1\end{bmatrix}^{\mathsf{T}}}_{N}\ ,\end{aligned} \tag{4}$$

where the spacings defined as $\Delta x = \frac{L}{N-1}$. Based on the vector representation of the corresponding function samples

$$\begin{aligned}f(x)\Big|_{x\in\mathbf{x}} &= \begin{bmatrix}f(x_0) & f(x_1) & \dots & f(x_N - 1)\end{bmatrix}^{\mathsf{T}} \\ &= \begin{bmatrix}f_0 & f_1 & \dots & f_{N-1}\end{bmatrix}^{\mathsf{T}} = \mathbf{f}\ ,\end{aligned} \tag{5}$$

and the Taylor series expansion of f_{-1} and f_1, the samples of the second order derivative can be expressed as

$$\frac{\partial^2}{\partial x^2}f(x)\Big|_{x\in\mathbf{x}} \approx \underbrace{\left[\frac{1}{\Delta x^2}\mathbf{B}_N^{(2)}\right]}_{\mathbf{L}_1^{(2)}}\mathbf{f} = \mathbf{L}_1^{(2)}\mathbf{f}\ , \tag{6}$$

where the N-th order quadratic matrix $\mathbf{B}_N^{(2)}$ is defined as

$$\mathbf{B}_N^{(2)} = \begin{bmatrix}2 & -1 & & & \\ -1 & 2 & -1 & & \\ & & \ddots & & \\ & & -1 & 2 & -1 \\ & & & -1 & 2\end{bmatrix}. \tag{7}$$

The higher order difference operators and partial operators can be derived in the same way based on the Taylor series expansion of the function samples [3].

In order to derive the corresponding finite *difference* equation of the plate, let us suppose that the finite argument space of plate's z directional displacement function will be N_x by N_y in directions x and y. Formulate now the vector representation of the displacement function samples as

$$\begin{aligned}\mathbf{p} = \big[u(x_1,y_1) \quad \dots \quad u(x_{N_x},y_1) \quad u(x_1,y_2) \quad \dots \\ u(x_{N_x},y_2) \quad \dots \quad u(x_{N_x},y_{N_y})\big]^{\mathsf{T}}\ ,\end{aligned} \tag{8}$$

and construct the "discrete" equation of motion

$$\left(\underbrace{D(\mathbf{L}_2^{(4)}) - T(\mathbf{L}_2^{(2)})}_{\mathbf{K}_p} - \omega^2\underbrace{\rho_p h\mathbf{I}}_{\mathbf{M}_p}\right)\mathbf{u} = \mathbf{F}\ , \tag{9}$$

where $\mathbf{L}_2^{(4)}$ and $\mathbf{L}_2^{(2)}$ matrices are the corresponding two dimensional difference representation of the biharmonic and the Laplacian operator and $\mathbf{I}$ is the identity matrix. Let us construct the "discrete" equation of motion for the air enclosure and the porous material in the same way. The sampled representation of the pressure function is defined as

$$\begin{aligned}\mathbf{p} = \big[p(x_1,y_1,z_1) \quad \dots \quad p(x_{N_x},y_1,z_1) \quad p(x_1,y_2,z_1) \\ \dots \quad p(x_{N_x},y_2,z_1) \quad \dots \quad p(x_{N_x},y_{N_y},z_{N_z})\big]^{\mathsf{T}}\ ,\end{aligned} \tag{10}$$

and let us express the equation of motion for the air layer as

$$\left[\underbrace{\mathbf{L}_3^{(2)}}_{\mathbf{K}_a} - \omega^2\underbrace{\left(-\rho\frac{1}{\kappa p_0}\right)\mathbf{I}}_{\mathbf{M}_a}\right]\mathbf{p} = \mathbf{0}\ . \tag{11}$$

where $\mathbf{L}_3^{(2)}$ matrix is the three dimensional representation of the Laplacian operator, and $\mathbf{I}$ is the identity matrix. The corresponding porous layer equation has the form

$$\left[\underbrace{\mathbf{L}_3}_{\mathbf{K}_o} + j\omega\underbrace{\left(-\sigma\phi\frac{1}{\kappa p_0}\right)\mathbf{I}}_{\mathbf{C}_o}\right]\mathbf{p} = \mathbf{0}\ . \tag{12}$$

2.3 Boundary conditions

Generally, Dirichlet (if the value of the variables are given) and Neumann (if the derivative of the value is given) boundary conditions are given for modelling problems. Based on a simple derivation these boundary conditions cause modification of corresponding values of the difference operator matrix values.

2.4 Coupling

Two main types of coupling are used. The first one defines the connection between the structure-fluid layers (like plate-air and plate-porous). In this case the z directional velocity of the fluid and the structure are the same. The governing equation are

$$\nabla p(\boldsymbol{r},t) = -\rho\frac{\partial}{\partial t}\boldsymbol{v}(\boldsymbol{r},t), \tag{13}$$

$$\nabla p(\boldsymbol{r},t) = -\sigma\phi\boldsymbol{v}(\boldsymbol{r},t)\ , \tag{14}$$

where both equations are the Euler's equation. These equations are transformed into finite difference equations and are used to calculate coupling matrices.

The second types of coupling defines the linear connections between the function values at the given points of the model. This boundary condition can describe, for example, if the i-th and the j-th element are connected (their displacement are the same for example) the corresponding equation will be $u_i - u_j = 0$. Let us define these kind of equations in the following form

$$\mathbf{Z\Phi} = \mathbf{0} \,, \tag{15}$$

where the matrix $\mathbf{\Phi}$ stands for the mixed variables (pressure and displacement) and the corresponding row (i-th and j-th column) of the $\mathbf{Z}$ matrix is the following

$$\mathbf{Z} = \begin{bmatrix} & \vdots & & \vdots & \\ \dots & 1 & \dots & -1 & \dots \\ & \vdots & & \vdots & \end{bmatrix} \leftarrow i\text{-th row} \,. \tag{16}$$

Since these kind of equations mean that some variables can be expressed as linear combination of others e.g. the expressed variables can be neglected. A transformation matrix $\mathbf{T}$ between the set of the original and the reduced variables can be introduced as

$$\mathbf{\Phi} = \mathbf{T\Phi'} \,, \tag{17}$$

where $\mathbf{\Phi'}$ is the reduced variable set.

2.5 Radiation

The calculation concept assumes a simple radiation schema as illustrated on Fig. 1. The radiating surface is rectangular, parallel to the x-y plane, radiates sound only to the half space and is baffled, all the other part of the coincident surface has zero displacement. In order to derive the radiation part of the theory, let us consider a radiating surface situated at $z = 0$. Express the pressure value $p(\boldsymbol{r})$ at any selected spatial point ($\boldsymbol{r}$) using Rayleigh's integral formula

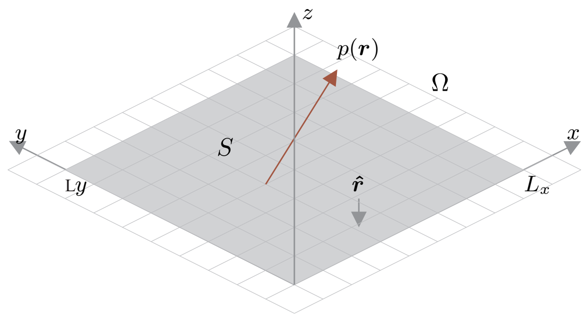

Figure 1: A radiating surface baffled in $x - y$ plane

$$p(\boldsymbol{r},\omega) = -2 \int_S \rho j \omega \hat{v}_z(\hat{\boldsymbol{r}},\omega) g(\boldsymbol{r},\hat{\boldsymbol{r}},\omega)\,\mathrm{d}\boldsymbol{S}(\hat{\boldsymbol{r}})$$

$$= 2\omega^2 \rho \int_S \hat{u}_z(\hat{\boldsymbol{r}},\omega) g(\boldsymbol{r},\hat{\boldsymbol{r}},\omega)\,\mathrm{d}\boldsymbol{S}(\hat{\boldsymbol{r}}) \,, \tag{18}$$

where $\hat{\boldsymbol{r}} \in \boldsymbol{S}$, $\hat{v}_z(\hat{\boldsymbol{r}},\omega)$ and $\hat{u}_z(\hat{\boldsymbol{r}},\omega)$ stand for the z-directional (normal) velocity and displacement of the surface points, $g(\boldsymbol{r},\boldsymbol{q})$ indicates the *Green's function* which is defined as

$$g(\boldsymbol{r},\boldsymbol{q},\omega) = \frac{1}{4\pi} \frac{e^{\frac{j\omega}{c}|\boldsymbol{r}-\boldsymbol{q}|}}{|\boldsymbol{r}-\boldsymbol{q}|} \,, \tag{19}$$

where c is the speed of sound. Using Rayleigh's equation (18) and combining with the definition of a linear shape function yields

$$p(\boldsymbol{r},\omega) = 2\omega^2 \rho \int_S \left(\sum_{k=1}^{N} \alpha_k(\hat{\boldsymbol{r}}) \hat{u}_z(\hat{\boldsymbol{r}}_k,\omega) \right) g(\boldsymbol{r},\hat{\boldsymbol{r}},\omega)\,\mathrm{d}\boldsymbol{S}(\hat{\boldsymbol{r}})$$

$$= 2\omega^2 \rho \sum_{k=1}^{N} \hat{u}_z(\hat{\boldsymbol{r}}_k,\omega) \int_S \alpha_k(\hat{\boldsymbol{r}}) g(\boldsymbol{r},\hat{\boldsymbol{r}},\omega)\,\mathrm{d}\boldsymbol{S}(\hat{\boldsymbol{r}}) \,, \tag{20}$$

where the $\alpha_k(\hat{\boldsymbol{r}})$ is the k-t shape function. If M different spatial points are assumed $\mathbf{r} = \begin{bmatrix} \boldsymbol{r}_1 & \boldsymbol{r}_2 & \dots & \boldsymbol{r}_M \end{bmatrix}^\mathsf{T}$ then

$$\mathbf{p}(\mathbf{r},\omega) = \omega^2 \rho \mathbf{R}_3(\mathbf{r},\hat{\mathbf{r}},\omega)\hat{\mathbf{u}}_z \,, \tag{21}$$

where

$$[\mathbf{R}_3(\mathbf{r},\hat{\mathbf{r}},\omega)]_{i,k} = 2 \int_S \alpha_k(\hat{\boldsymbol{r}}) g(\boldsymbol{r}_i,\hat{\boldsymbol{r}},\omega)\,\mathrm{d}\boldsymbol{S}(\hat{\boldsymbol{r}}) \,. \tag{22}$$

The numerical integration can be made by means of Gauss-Legendre quadrature.

2.6 Final model

After expressing the related matrices of all layers (taking into account the boundary conditions of each layer) and calculating the coupling and radiation matrices, the final equation of motion has to be solved. Since the radiation matrix is frequency dependent, the modal decomposition based solution of equation is not possible.

3 G1 flat loudspeaker

Panphonics' G1 loudspeaker is an electrostatic audio device. The cross sectional view of the loudspeaker is depicted in Fig. 2. This cross sectional inner structure is homogeneous to y direction. In the middle of all cells a special foil (conductor) is placed between two porous electrostatic thin layers (stators). The driving signal is connected to the foil and the bias voltages are connected to the stators. Due to the electric field between the foil and the stators the foil starts to move, generates air flow trough the stators and the porous cover layers. The foil of G1 is modelled as a plate with only z directional displacement considered. The upper and lower porous cover layers were modelled as plate structures and the air flow inside the layers was modelled as a porous layer.

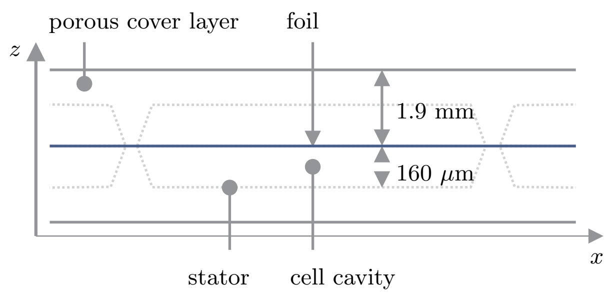

Figure 2: Cross-sectional view of G1 loudspeaker

3.1 Modelling results

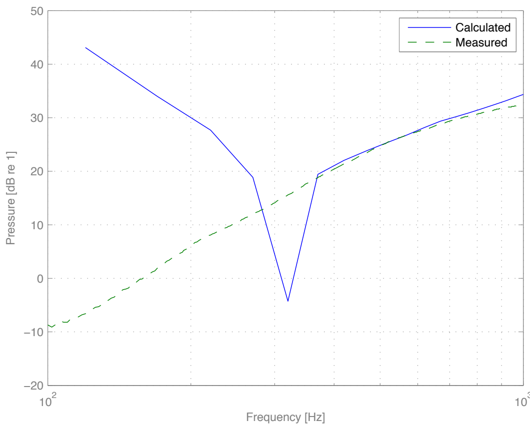

Figure 3: Pressure level at 1 m from loudspeaker

The measured and the calculated pressure at 1 m from the loudspeaker can be seen in 3. It is important to note that the driving conditions are unknown at the measured case so only the shape of the curves can be compared. Since the modelling conditions are different from the measuring conditions, the low-frequency results show larger deviation.

However, the model calculation proved the tendency of the foil displacement at low and higher frequencies [4]. At low frequency the panel has a "global" displacement (depicted in Fig. 4) which generates a near field local pressure stream. Due to the half-space calculation assumption, the model cannot take itto account and that is why one can see high pressure level at low frequencies. At higher frequencies only the "local" displacement dominates (see in Fig. 5)

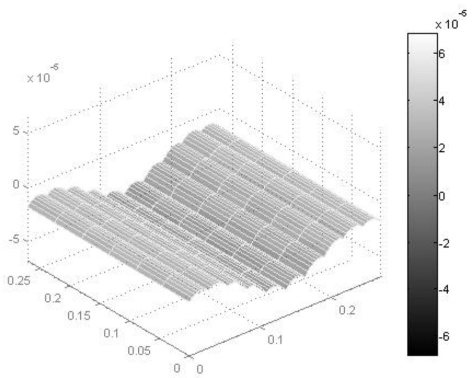

Figure 4: Displacement of the foil at 120 Hz (calculation)

4 Conclusion

Due to the inaccuracy of the initial parameter of the G1 (material parameters) and the indefinite measuring conditions, the results show high variation. In order to get more reliable results a detailed verification measurement is to be done and model updating is planned.

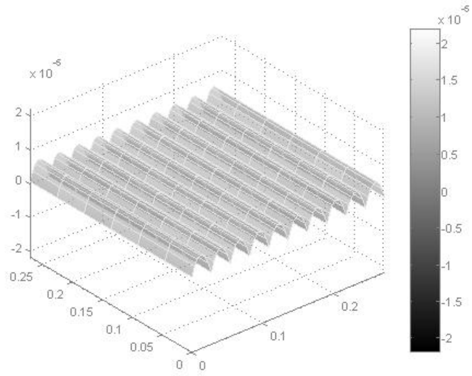

Figure 5: Displacement of the foil at 970 Hz (calculation)

Acknowledgments

The work has been done in the framework of the European Union funded project Intelligent Materials for Noise Reduction (InMAR).

References

[1] L. Meirovitch, "Elements of Vibration Analysis", McGraw-Hill Inc., New York (1975)

[2] Z. E. A . Fellah, M. Fellah, N. Sebaa and W. Lauriks, C. Depollier "Measuring flow resistivity of porous materials at low frequencies range via acoustic transmitted waves", *Acoustical Society of America Journal*, vol. 119 1926-1928 (2006)

[3] Wikipedia, *Finite difference — Wikipedia, The Free Encyclopedia,* "[Online; accessed 7-May-2008]"

[4] A. Kelloniemi, V. Mellin, S. Finnveden, R. Guastavino and P. Göransson "Mechanical study of a plane wave transducer for active noise", *INTER-NOISE 2007, Istanbul, Turkey*